HHS Public Access

Author manuscript

Neuroscience. Author manuscript; available in PMC 2019 February 10.

Published in final edited form as:

Neuroscience. 2018 February 10; 371: 126–137. doi:10.1016/j.neuroscience.2017.11.053.

α1b-Adrenergic Receptor Localization & Relationship to the D1-Dopamine Receptor in the Rat Nucleus Accumbens

Darlene A. Mitrano[a,b,*], **Kelsey Jackson**[a,b,1], **Samantha Finley**[b,2], and **Allison Seeley**[b,3]

[a]Department of Molecular Biology & Chemistry, Christopher Newport University, 1 Avenue of the Arts, Newport News, Virginia 23606

[b]Program in Neuroscience, Christopher Newport University, 1 Avenue of the Arts, Newport News, Virginia 23606

Abstract

The α1-adrenergic receptors (α1ARs) have been implicated in numerous actions of the brain, including attention and wakefulness. Additionally, they have been identified as contributing to disorders of the brain, such as drug addiction, and recent work has shown a role of these receptors in relapse to psychostimulants. While some functionality is known, the actual subcellular localization of the subtypes of the α1ARs remains to be elucidated. Further, their anatomical relationship to receptors for other neurotransmitters, such as dopamine (DA), remains unclear. Therefore, using immunohistochemistry and electron microscopy techniques, this study describes the subcellular localization of the α1b-adrenergic receptor (α1bAR), the subtype most tied to relapse behaviors, as well as its relationship to the D1-dopamine receptor (D1R) in both the shell and core of the rat nucleus accumbens (NAc). Overall, α1bARs were found in unmyelinated axons and axon terminals with some labeling in dendrites. In accordance with other studies of the striatum, the D1R was found mainly in dendrites and spines; therefore, colocalization of the D1R with the α1bAR was rare postsynaptically. However, in the NAc shell, when the receptors were co-expressed in the same neuronal elements there was a trend for both receptors to be found on the plasma membrane, as opposed to the intracellular compartment. This study provides valuable anatomical information about the α1bAR and its relationship to the D1R and the regulation of DA and norepinephrine (NE) neurotransmission in the brain which have been examined previously.

Keywords

alpha1-adrenergic receptors; D1-dopamine receptors; nucleus accumbens

[*]Corresponding Author: Darlene A. Mitrano, Ph.D., Christopher Newport University, Department of Molecular Biology & Chemistry, 1 Avenue of the Arts, Newport News, Virginia 23606, darlene.mitrano@cnu.edu, Phone: (757) 594-8632, Fax: (757) 594-7356.

[1]Present contact info: Kelseyannehummel@gmail.com

[2]Present contact info: NeuroGrow Brain Fitness Center, McLean, VA 22102; sfinley@neurogrow.com

[3]Present contact info: School of Public Health, University of Michigan; aseeley.m@gmail.com

Introduction

Psychostimulant abuse and addiction remains a societal problem in the United States. The latest statistics from the National Survey on Drug Use and Health indicate that slightly less than one million people over the age of 12 report having a cocaine use disorder (NSDUH, 2016). Additionally, about 11% of American children have been diagnosed with Attention Deficit Hyperactivity Disorder (ADHD), with over 70% being treated with stimulant medications (Visser et al., 2014). A problem that has arisen is the misuse of ADHD medications for non-medical purposes, with recent surveys finding approximately 1.7 million individuals in the United States abusing stimulant drugs without a prescription (NSDUH, 2016). A goal in understanding the mechanisms behind dependency and abuse of psychostimulant drugs is to explore relevant underlying circuitry, receptors & neurochemistry in the brain.

The Mesocorticolimbic Pathway, Norepinephrine & Dopamine

The mesocorticolimbic pathway, encompassing the ventral tegmental area (VTA), nucleus accumbens (NAc) and prefrontal cortex (PFC), are interconnected structures in the brain that allow us to experience pleasure from natural rewards and from drugs that manipulate levels of two catecholamine neurotransmitters, dopamine (DA) and norepinephrine (NE). The PFC controls key cognitive functions such as planning and impulse control, which are disrupted by disorders such as ADHD and drug addiction (Arnsten & Li, 2005; Hains & Arnsten, 2008). The NAc, divided into the core & shell, is critical for experiencing pleasurable feelings and the euphoric properties of stimulants (Wise & Bozarth, 1985, 1987; Zahm & Brog, 1992; Meredith et al., 1996). DA and NE, and their transporters and receptors, have been shown to play a role in regulating pathological changes in disorders such as ADHD and stimulant addiction (Ritz et al., 1988; Darracq et al., 1998; Pan et al., 2004; Weinshenker & Schroeder, 2007; Heal et al, 2009). For example, cocaine, amphetamine and related compounds, such as the prescription drug methylphenidate (for treating ADHD), act by increasing levels of synaptic NE and/or DA, which in turn activate the various subtypes of NE and DA receptors (Ritz et al., 1988; Ritz & Kuhar, 1989; Heal et al., 2009).

G-protein coupled receptors (GPCRs) responding to dopamine (D1Rs) and norepinephrine (α1ARs) are abundant within the mesocorticolimbic system and are essential for both the therapeutic efficacy and addictive properties of stimulants (Darracq et al., 1998; Drouin et al., 2002; Heal et al., 2009; Mitrano et al., 2012, 2014; Schmidt & Weinshenker, 2014). There are three classes of noradrenergic receptors, α1-, α2- and β-adrenergic receptors. Amongst the α1-adrenergic receptors (α1ARs), there are three subtypes, α1a, α1b and α1d (Bylund et al., 1994; Zhong & Minneman, 1999). While the subtypes of the receptor and some of their properties have been known for some time (Bylund et al., 1994; Zhong & Minneman, 1999; Chalothorn et al., 2002), their exact function and localization in various brain regions are still being elucidated. A major roadblock in understanding the functionality of each of the α1AR subtypes in the brain is the fact that subtype-specific pharmacological agents have yet to be developed (Giardina et al., 1996, 2003; Aono et al., 2015). Therefore, most studies addressing the functions of α1AR subtypes have used knockout (KO) animals

(Drouin et al., 2002; Auclair et al., 2002), transfected cells (Vicentic et al., 2002), or animals that overexpress the receptors (Zuscik et al., 2000; Yun et al., 2003).

There is evidence for the α1ARs playing a role in addictive behaviors to stimulant drugs, namely in relapse or reinstatement of drug-seeking behavior (Zhang & Kosten, 2005; Weinshenker & Schroeder, 2007; Gaval-Cruz & Weinshenker, 2009; Schroeder et al., 2013). For example, the α1AR antagonist prazosin attenuates cocaine-induced reinstatement (Zhang & Kosten, 2005), while the dopamine β-hydroxylase inhibitor nepicastat blocks cue-induced, cocaine-induced and stress-induced reinstatement to cocaine-seeking (Schroeder et al., 2013). Using *in vivo* microdialysis in the NAc, it was shown that activation of presumed presynaptic α1ARs with the α1AR agonist methoxamine can decrease DA efflux (Saisuga et al., 2012), and when exposed to cocaine, NE release in the PFC can indirectly control DA transmission to the NAc (Drouin et al., 2002; Zhang & Kosten, 2005). Specific focus has turned to the α1bAR subtype in relation to stimulant effects and regulation of dopamine. For example, Drouin et al. (2002) showed α1bAR knockout mice had reduced locomotor responses to amphetamine, cocaine and morphine. Auclair et al. (2002) showed that dopamine-induced increases in the NAc were significantly decreased in α1bAR KO mice following amphetamine administration, as opposed to stimulating the α1bARs which resulted in increased DA-mediated locomotor responses to amphetamine (Villegier et al., 2003). These studies, just to name a few, indicate a relationship between NE, α1bARs, DA and D1Rs in the NAc in relation to neural and psychological responses to psychostimulants.

The subcellular localization of the α1AR has been characterized previously in the NAc (Mitrano et al., 2012), but localization of the specific subtype α1bAR has not been described, though suggested in some studies (Saisuga et al., 2012). If we are to truly gain an understanding of their role and relationship to DA and dopamine receptors, the subcellular and subsynaptic localization of the α1bAR is necessary. Additionally, even though the anatomical localization of the D1Rs has been shown in the dorsal striatum and PFC (Levey et al., 1993; Hersch et al., 1995; Dumartin et al., 1998; Mitrano et al., 2014), their relationship to the specific adrenergic receptor, α1bAR, has yet to be established in the NAc.

Therefore, this study aimed to define the subcellular and subsynaptic localization of both the α1bAR and the D1R in the core and shell of the rat NAc using immunohistochemistry and electron microscopic (EM) techniques. Next, using double labeling techniques at the EM level, the degree of finding these receptors in the same neural elements or glia was assessed. Based on previous work on the localization of the α1ARs (Mitrano et al., 2012; 2014), it was hypothesized that there would negligible colocalization of the α1bAR and the D1R. Overall, the majority of α1bARs were found presynaptically, while D1Rs were located mainly postsynaptically. Generally, minimal colocalization of these two receptors was detected in most neuronal elements as well as glial processes.

Experimental Procedures

Animal treatment for immunohistochemistry

All procedures were approved by the Institutional Animal Care and Use Committee of Christopher Newport University. In total, 13 male adult Sprague-Dawley rats (Charles River

Laboratories, Wilmington, MA; weighing approximately 200–300 grams) were used for this study. Rats were anesthetized with a ketamine (100mg/kg) and butorphanol (2mg/kg) cocktail and transcardially perfused with 4% paraformaldehyde containing 0.1% glutaraldehyde (Electron Microscopy Sciences (EMS), Hatfield, PA). Brain tissue was removed and postfixed for 24 hours in 4% paraformaldehyde and cut into 60μm sections on a vibrating microtome. Prior to immunohistochemical labeling, all tissue was exposed to 1% $NaBH_4$.

Primary antibodies for immunohistochemistry

Table 1 lists the primary antibodies and their concentrations used in this study. The specificity of the D1R antibody has been characterized and published on previously (Levey et al., 1993; Hersch et al., 1995; Mitrano et al., 2014). More recently, Stojanovic et al. (2017) used brain tissue from D1R knockout and wild-type mice and through the use of immunohistochemistry, western blot and immunoprecipitation followed by mass spectrometry analysis, showed that this D1R antibody (produced by Sigma-Aldrich, St. Louis, MO) is specific for the receptor. The α1bAR antibody (Abcam, Cambridge, MA) was tested previously in HEK-293 cells and showed labeling in Western blot analysis only when the cell was transfected with α1bAR DNA. No bands were present when the cells were transfected with mock-DNA or DNA of another receptor (data not shown; Mitrano et al., 2010; 2014).

Single pre-embedding immunoperoxidase labeling for α1bARs and D1Rs

In order to determine the working concentrations of both of the primary antibodies, serial dilutions were tested using immunohistochemical procedures for light microscopy (based on methods described in Mitrano & Smith, 2007). After $NaBH_4$ treatment, sections were incubated for 1 hour at RT in phosphate-buffered saline (PBS; pH 7.4) containing 10% normal goat serum (NGS; Vector Laboratories, Burlingame, CA), 1% Bovine Serum Albumin (BSA; Sigma), and 0.3% Triton, followed by the primary antibody solution containing 1% NGS, 1% BSA, and 0.3% Triton in PBS for 24 hours at RT. Sections were then incubated in secondary biotinylated goat anti-rabbit IgGs for the α1bAR or goat anti-rat IgGs for the D1R (1:200; Vector) for 90 minutes and then incubated for another 90 minutes with the avidin-biotin peroxidase complex (ABC Kit; 1:100; Vector). Finally, the sections were washed in PBS and Tris buffer (50 mM; pH 7.6) and transferred to a solution containing 0.025% 3,3-diaminobenzidine tetrahydrochloride (DAB; Sigma), 10 mM imidazole, and 0.005% hydrogen peroxide in Tris buffer for 10 minutes. Sections were rinsed in PBS, mounted onto gelatin-coated slides, dehydrated, and then coverslipped with Cytoseal (ThermoFisher Scientific, Waltham, MA). Tissue was examined using a light microscope (data not shown), and final concentrations were determined based on labeling patterns observed in previous studies (Levey et al., 1993; Hersch et al., 1995; Mitrano et al., 2012, 2014).

Single pre-embedding immunoperoxidase labeling for α1bARs and D1Rs for electron microscopy

Tissue used for labeling the α1bAR was incubated at the same time, while tissue used for labeling the D1R were completed at the same time to ensure consistency in the conditions of

the solutions used. Following $NaBH_4$ treatment, sections were placed in a cryoprotectant solution for 20 minutes, frozen at −80°C for 20 minutes, returned to a decreasing gradient of cryoprotectant solutions, and rinsed in PBS. Sections were then incubated in primary and secondary antibody solutions identical to those described above with two exceptions, omission of Triton and incubation in the primary antibody for 48 hours at 4°C. After the DAB reaction, the tissue was rinsed in PB (0.1M, pH 7.4) and treated with 1% OsO_4 (EMS) for 20 minutes. Tissue was then dehydrated with increasing concentrations of ethanol. When exposed to 70% ethanol, 1% uranyl acetate (EMS) was added to the solution for 35 minutes to increase the contrast of the tissue at the electron microscopic level. After dehydration, sections were treated with propylene oxide (EMS) and embedded in Durcupan ACM resin (Sigma) overnight, mounted onto slides, and placed in a 60°C oven for 48 hours. Separate samples of the nucleus accumbens core and medial shell (based on coordinates from Paxinos & Watson, 1998), were cut out of the larger sections, mounted onto resin blocks, and cut into 60-nm sections with an ultramicrotome (Leica Reichert Ultracut S). The 60-nm sections were collected on copper mesh grids (EMS) stained with lead citrate (EMS) for 5 minutes to enhance tissue contrast, and examined on a transmission electron microscope. Transmission electron microscopes used were the JEOL-1010 (University of Richmond); JEOL-1011 (Emory University) and JEOL-1230 (Virginia Commonwealth University).

Analysis of single pre-embedding immunoperoxidase labeling for α1bARs and D1Rs

Data for single immunoperoxidase labeling was collected from 20 blocks of tissue, one block/animal in the medial NAc shell and one block/animal in the NAc core, immunostained for either the α1bAR or the D1R in five rats each. Serial ultrathin sections taken from each of the blocks when the interface of resin and labeled tissue were visible. Thirty-forty electron micrographs of randomly selected immunoreactive elements were imaged at 40,000x and saved with a CCD camera controlled by Digital Micrograph or AMT Image Capture (version 5.42.498). Some of the digitally acquired electron micrographs were adjusted for brightness or contrast in Adobe Photoshop (version 12.0.4x32). Micrographs were then compiled into figures using Adobe Illustrator (version 15.0.2). Labeled elements were categorized as dendrites, spines, unmyelinated axons, myelinated axons, axon terminals or glia, based on ultrastructural features described by Peters et al. (1991). Spines are usually mushroom-shaped, have a visible postsynaptic density and are usually opposed to an axon terminal, identified by the presence of vesicles. Unmyelinated axons are small, regular, circular elements that are relatively smooth in shape, travel straight in the neuropil when seen in longitudinal plane and are frequently clustered, forming a bundle. Dendrites display different sizes and shapes, contain mitochondria, stacks of endoplasmic reticulum and often receive synaptic contacts. Glial processes are usually thin, have an irregular shape and are not found in bundles. The total number of labeled elements was summed for each animal and then the percentage of each of the above named elements was determined for each animal. The mean of the percentages for each element was calculated (+/− SEM) across the 5 animals in each group (n=5 for α1bAR NAc core; n=5 for α1bAR NAc shell; n=5 for D1R NAc core; n=5 for D1R NAc shell).

Significant differences between the means of identified elements were assessed by using IBM SPSS Statistics (version 24). It should be noted that non-independent data was used for

statistical analyses and therefore results apply to the animals sampled, not necessarily applicable to the population of Sprague-Dawley animals. First, for each receptor, a one-way ANOVA was run to determine whether the mean percentage of each of the labeled elements identified differed between the NAc core and shell; this also included Levene's test for homogeneity of variances. Next, in order to determine whether the percentage of labeled elements differed between the two receptor types (from the 5 animals in each group), a one-way ANOVA followed by Tukey's post-hoc test was done. In other words, the mean percentage of labeled dendrites, spines, unmyelinated axons, etc., labeled for the α1bAR in the NAc core, the α1bAR in the NAc shell, the D1R in the NAc core and the D1R in the NAc shell were compared; this also included Levene's test for homogeneity of variances.

Double pre-embedding labeling for α1bARs and D1Rs for electron microscopy

As described above, for single pre-embedding labeling, tissue was double-labeled for both receptors in the combinations described below at the same time. Following $NaBH_4$ treatment, sections went through a series of cryoprotectant rinses. Tissue was then placed in a preincubation solution containing 5% dry milk and PBS for 30 minutes at RT. Following rinses in a TBS (tris-buffered saline)-gelatin buffer (pH 7.6), sections were transferred to a solution that contained a mixture of the D1R and α1bAR antibodies and incubated overnight at RT (based on methods in Mitrano & Smith, 2007). In order to account for any false positive labeling (as background labeling is common when revealing an antibody with gold-conjugated secondaries), the double-labeling reaction was performed twice, once with the primary antibodies for α1bAR revealed with immunogold and D1R with immunoperoxidase, as well as the reverse. The next day, the tissue was exposed to the two secondaries for 2hrs at RT. When revealing the D1R with immunogold, secondary antibodies were goat anti-rat IgGs conjugated with 1.4 nm gold particles (1:100; Nanoprobes, Yaphank, NY); when revealing with immunoperoxidase method (described above), goat anti-rat biotinylated IgGs were used (Vector). For revealing the α1bAR, goat anti-rabbit IgGs conjugated with 1.4 nm gold particles were used for immunogold and goat anti-rabbit biotinylated IgGs were used for immunoperoxidase. Following rinses with TBS-gelatin and $C_2H_3NaO_2$, an HQ Silver Enhancement kit (Nanoprobes) was used for intensification of gold particles (to create ~40nm gold particles visible under the EM) for 4 min at RT in the dark. Following silver intensification, ABC, and DAB procedures were performed as described above. Immediately following the DAB reaction, sections were subjected to osmification, dehydration and resin embedding protocols described previously, with two exceptions: 0.5% OsO_4 was used for 10min and exposure to 70% ethanol with 1% uranyl acetate for 10min.

Analysis of double pre-embedding labeling of α1bARs and D1Rs for electron microscopy

Data were collected from a total of 21 blocks (n=5 for D1R revealed with immunoperoxidase, α1bAR revealed with immunogold, for both the NAc core and shell; n=5 for D1R immunogold, α1bAR immunoperoxidase in the NAc core; n=6 for D1R immunogold, α1bAR immunoperoxidase in the NAc shell). Serial ultrathin sections were taken from each of the blocks when the interface of resin and labeled tissue were visible. Thirty- forty electron micrographs were taken from each animal for each receptor/secondary antibody combination at 40,000x in fields where both immunoperoxidase and immunogold

labeling were both visible, and images were saved with a CCD camera controlled by Digital Micrograph or AMT Image Capture (version 5.42.498).

Some of the digitally acquired electron micrographs were adjusted for brightness or contrast in Adobe Photoshop (version 12.0.4x32). Micrographs were then compiled into figures using Adobe Illustrator (version 15.0.2). For these reactions, the elements for the receptor revealed with immunoperoxidase were counted first, followed by the number of those elements that also contained immunogold labeling. The percentage of double-labeled elements was calculated for each animal and then averaged across animals. In addition to determining the degree of colocalization of the two receptors, the receptor revealed with immunogold was further analyzed in both double- and single-labeled elements to describe its subsynaptic localization. First, the gold particles were classified as either intracellular (INT; inside the element, not touching the plasma membrane) or plasma-membrane bound (PMB; touching the plasma membrane of the element). PMB gold particles were further classified into three categories: perisynaptic (touching or within a 20-nm range of the edges of a postsynaptic density), synaptic (in contact with the main body of the postsynaptic density), or extrasynaptic (on the plasma membrane but not associated with a synapse).

It should be noted that non-independent data was used for statistical analyses and therefore results apply to the animals sampled, not necessarily applicable to the population of Sprague-Dawley animals. Using SPSS, a series of analyses were done. First, the mean percentage of colocalization of the receptors amongst the different elements (dendrites, spines, unmyelinated axons, axon terminals and glia) was compared within each brain region using two one-way ANOVAs (one for the NAc core and one for the NAc shell), followed by Tukey's post hoc tests and Levene's test for homogeneity of variance. In order to determine that neither receptors' secondary antibody yielded false positives, two one-way ANOVAs with Tukey's post-hoc test was run (for each combination) to determine if there was any statistically significant differences in the degree of colocalization of the α1bAR and D1R when the secondary antibody conjugates were reversed (i.e. immunogold vs. immunoperoxidase).

Next, when each receptor was revealed with immunogold, the amount of intracellular versus PMB gold particles was compared by using two one-way ANOVAs, Tukey's post hoc test and Levene's test for homogeneity of variance. One ANOVA was done for comparing the subsynaptic localization of the immunogold particles representing the α1bAR in both the core and shell and the other ANOVA was done for the D1R in both the core and shell. Two-way ANOVAs were used to determine statistical differences between the receptors in the amount of immunogold labeling found intracellularly or PMB in all of the elements examined.

To determine if the subsynaptic localization of each receptor differed in double labeled elements versus single labeled elements, as seen in other brain regions such as the PFC (Mitrano et al., 2014), the distribution of intracellular versus PMB gold particles was compared, using a series of one-way ANOVAs and Levene's test for homogeneity of variance.

Controls for Immunohistochemistry

To further support the specificity of each primary antibody, for the single labeling experiments, two controls were set up. One used the wrong secondary; for example when using the α1bAR primary antibody (made in rabbit), select sections were exposed to the wrong secondary (biotinylated goat anti-guinea pig IgGs), and no labeling was found for both the α1bAR and D1R (as done in Mitrano et al., 2014). Additionally, as a negative control, the primary antibody was omitted, resulting in no labeling as well (data not shown).

For double pre-embedding experiments, controls consisted of omitting one of the primary antibodies for the α1bAR or the D1R, but exposing tissue to both secondaries, the HQ kit and ABC. No labeling was present when examined at the EM for any receptor for which the primary antibody was omitted, further confirming the specificity of the secondary antibodies.

Results

Subcellular localization of α1bARs and D1Rs in the NAc Core and Shell

As is displayed in Figure 1A, the α1bARs and D1Rs have different subcellular localizations within the NAc core and shell. The α1bAR was found mainly in unmyelinated axons and axon terminals (~55% of total labeled elements counted, and ~15%, respectively), with some labeling in dendrites and spines (~25–30% and ~5%, respectively) and glial elements (~5–10%; Figure 1B and C). There was no significant effect of region of the NAc when analyzing the distribution of the α1bAR in the core versus shell ($p>0.05$ for all elements). Additionally, no significant differences were found from Levene's test of homogeneity of variances for this comparison.

In contrast, the bulk of labeling for the D1R was found mainly in dendrites and spines (~50–55% and ~15% of total labeled elements counted, respectively), with some labeling in unmyelinated axons (~45%) and very little labeling found in axon terminals, myelinated axons and glial elements (all less than 10%; Figure 1A and D). There was no significant effect of region of the NAc when analyzing the distribution of the D1R in the core versus shell ($p>0.05$ for all elements). Levene's test for homogeneity of variances was only significant when looking at glial elements, however, this was taken into account by the ANOVA.

When comparing the pattern of labeling between receptors, there was a main effect of receptor type seen for all elements. There were significantly more D1R-containing dendrites than α1bAR-labeled dendrites in the core and shell ($F_{3,16}= 9.37$, $p<0.01$). Significantly more spines contained D1R than α1bAR in both the core and shell ($F_{3,16}= 30.28$, $p<0.001$). On the other hand, there was a significantly higher percentage of unmyelinated axons ($F_{3,16}= 4.26$, $p<0.05$), axon terminals ($F_{3,16}=11.97$, $p<0.001$) and glial elements ($F_{3,16}= 8.05$, $p<0.01$) containing the α1bAR, compared to the D1R. Levene's test showed homogeneity of variances except for myelinated axons. This was taken into account in the ANOVA and Tukey HSD performed. No further analysis was done on myelinated axons due to such a small number examined and wide variance between subjects.

Relationship of α1bARs and D1Rs in the NAc

Figure 2A represents the average percentage of α1bAR containing elements (revealed using pre-embedding immunoperoxidase) that also have labeling for the D1R (revealed using pre-embedding immunogold; Figures 2B–D). In both the NAc core and shell, about 25–30% of dendrites that contained labeling for the α1bAR also contained immunogold labeling for the D1R; ~10% of spines were double labeled; less than 10% of unmyelinated axons and axon terminals and ~10% of glial elements contained both receptors. Within the NAc core, a statistical difference was found amongst the percentages of double labeled elements ($F_{4,20}$=6.55, p<0.01). Post hoc tests revealed a greater proportion of dendrites labeled for both the α1bAR and D1R than unmyelinated axons (p<0.01); axon terminals (p<0.01) and glial elements (p<0.01). Levene's test showed homogeneity of variance. Almost the same results were seen within the NAc shell ($F_{4,25}$=3.68, p<0.05), where post hoc tests revealed that there were significantly more dendrites containing both the α1bAR and D1R than unmyelinated axons (p<0.05) and axon terminals (p<0.05). Levene's statistic did show significance when testing homogeneity of variance, but this was taken into account in the Tukey HSD.

As a control and as a means of providing increased validity to the findings above, we analyzed the co-localization of the D1R and α1bAR by reversing the experimental procedures described above. Figures 2E and F are representative electron micrographs of the NAc core and shell, respectively, when the secondary to reveal each receptor was reversed; in other words, the α1bAR was revealed using pre-embedding immunogold and the D1R was revealed using pre-embedding immunoperoxidase. When the conjugates of secondary antibodies were reversed, there were no significant differences seen in the percentage of double-labeled elements, in both the NAc core and shell (data not shown). An ANOVA showed no effect of secondary antibody conjugate within all element groups; for dendrites ($F_{3,17}$=2.38, p=0.11), spines ($F_{3,17}$=0.38, p=0.77), unmyelinated axons ($F_{3,17}$=0.79, p=0.52), axon terminals ($F_{3,17}$=1.83, p=0.18), and glial elements ($F_{3,17}$=1.82, p=0.18). This indicates that either secondary would have given the same results.

Subsynaptic Localization of the α1bAR and D1R in the NAc Core & Shell

When either receptor was labeled with a gold-conjugated secondary antibody, the gold particles were first analyzed as being INT or PMB, as described above. Then, PMB gold particles were further classified as either extrasynaptic, perisynaptic, or synaptic to either a putative asymmetric or symmetric synapse. Figures 3A and 3B display histograms summarizing the percentage of gold particles found intracellularly for the α1bAR (3A) or D1R (3B) in elements solely containing immunogold labeling for one of the two receptors in the NAc core and shell. When examining just the localization of the α1bAR, there were significantly more INT receptors than PMB receptors found in dendrites ($F_{3,16}$=44.99, p<0.001), with no differences found between the core and shell. The opposite was found for unmyelinated axons, with significantly fewer INT receptors than PMB ones ($F_{3,16}$=16.17, p<0.01), again with no differences between the core and shell. For axon terminals, in the NAc shell, there were significantly more intracellular α1bARs than PMB α1bARs ($F_{3,16}$=13.58, p<0.001). There was not a statistical difference in INT vs. PMB receptors in the NAc core for axon terminals. Likely due to the limited number of spines and glial

elements labeled for the α1bAR, no statistical differences between INT vs. PMB subsynaptic localization was found in either area of the NAc. Levene's test showed homogeneity of variance in the distribution of the α1bAR data. When examining the subsynaptic localization of just the D1R, no statistically significant differences were found in the percentages of intracellular vs. PMB receptors nor between the NAc core and shell (both comparisons showed homogeneity of variance).

When comparing the receptors to each other, a series of two-way ANOVAs was run with receptor and NAc region as the factors and the percent of intracellular gold particles for each element as the dependent variable. For dendrites, there was a main effect of receptor ($F_{1,17}$=49.55, $p<0.01$), indicating that regardless of NAc region, there were significantly more α1bARs found intracellularly compared to the D1R. For spines, unmyelinated axons, axon terminals and glial elements, there was no effect of region nor receptor and no interaction between the two factors.

Analysis of localization on the plasma membrane of the α1bAR and D1R revealed almost all labeling for both receptors was extrasynaptic. For D1Rs, there was a trend for slightly more perisynaptic and synaptic labeling at both asymmetric and symmetric synapses.

Due to the pattern seen in the prefrontal cortex, in which α1bARs were found to be more intracellular when found in D1R-expressing dendrites compared to dendrites only containing the α1bAR (Mitrano et al., 2014), the same analysis was done for the NAc core and shell. The pattern of subsynaptic labeling (proportion of INT vs. PMB) in elements that only contained immunogold labeling for the α1bAR vs. elements that had labeling for both the α1bAR and D1R and vice versa was compared. For the α1bAR, in the NAc shell (Figure 3C), there was a main effect of the percentage of intracellular α1bAR labeling in unmyelinated axons ($F_{1,8}$=7.95, $p<0.05$) and axon terminals ($F_{1,8}$=10.50, $p<0.05$). This indicates that when the α1bAR was found with the D1R in presynaptic elements, the α1bAR tended to be PMB (Levene's significant difference in variances was taken into account by the ANOVA). No statistically significant differences were found within the NAc core (data not shown), although there was a trend towards increased PMB expression of the α1bAR in all elements examined.

For the D1 receptor in the NAc shell (Figure 3D), there was a main effect of colocalization with α1bAR in spines ($F_{1,10}$=13.86, $p<0.01$) and axon terminals ($F_{1,10}$=10.34, $p<0.01$). Levene's statistic was only significant for unmyelinated axons, which was taken into account by the ANOVA. This indicates that when co-localized with the α1bAR, the D1R was found more often on the plasma membrane. No statistically significant differences were found within the NAc core (data not shown), although there was also a trend towards increased PMB expression of the D1R in spines and axon terminals.

Discussion

Overall, this study showed that the majority of α1bARs were found presynaptically in unmyelinated axons and axon terminals, with some labeling in postsynaptic dendrites. In dendrites and axon terminals, the α1bAR was found mainly intracellularly, while in

unmyelinated axons, it was mainly on the plasma membrane. In contrast, D1Rs were located mainly postsynaptically in dendrites and spines, with some labeling in unmyelinated axons. Additionally, in dendrites and spines, the D1R was mainly found on the plasma membrane. Generally, minimal colocalization of these two receptors was detected in most neuronal elements as well as glial cells. When they were found together, both the α1bARs and D1Rs tended to be located on the plasma membrane. This study provides new anatomical evidence supporting observations of functional interactions between these receptors described below.

Relationship between NE and DA

The association between dopamine and norepinephrine has been studied for years in relation to normal states of the brain, such as attention, wakefulness, reward and stress (Trovero et al., 1994; Pan et al., 2004; Arnsten & Li, 2005; Weinshenker & Schroeder, 2007). These catecholamine neurotransmitters, along with their receptors, have also been studied in disease states, such as depression, anxiety, drug addiction and ADHD (Ritz et al., 1988; Darracq et al., 1998; Pan et al., 2004; Arnsten & Li, 2005; Weinshenker & Schroeder, 2007; Heal et al, 2009; Goto et al., 2010; Atorzi et al., 2016). In order to further our understanding of the relationship between these receptors and neurotransmitters, functional and anatomical studies are needed in order to understand the normal and disordered states of the brain. For example, in the medial PFC, infusion of NE resulted in an increase in extracellular DA that was blunted by the α1AR antagonist prazosin, while infusion of DA into the same area resulted in increases in extracellular NE, inhibited by a D1R antagonist (Pan et al., 2004). In cultured cortical neurons, the α1AR agonist methoxamine accelerated the resensitization of DA stimulated D1Rs as measured by cAMP levels, which was blunted by prazosin (Trovero et al., 1994). These studies, to describe a few, correlate with the high degree of colocalization of the α1ARs and D1Rs in PFC cortical dendrites as shown by Mitrano et al. (2014), as they describe a relationship that indicates that there may be receptor-receptor interactions yet to be determined at the molecular level. These also lay a foundation for a better understanding of how these receptors might be mediated by new drug treatments or drugs of abuse which target the PFC.

α1bAR and D1Rs in the NAc

The major sources of NE to the NAc include the locus coeruleus (LC) as well as the A1/A2 brainstem nuclei (reviewed in Weinshenker & Schroeder, 2007; Atorzi et al., 2016). Past studies that have examined the localization of the α1AR, using a pan-α1AR antibody (detecting all three subtypes) showed the majority of the receptors being presynaptic in both the core and shell of the NAc (Mitrano et al., 2012). Additionally, within the NAc it was found that α1ARs were found on glutamatergic and dopaminergic axon terminals; however, it remains unknown whether a particular subtype of the α1AR would be found more prominently on one of the different types of terminals. This would be especially important considering it was found that stimulating the LC causes NE release in the VTA, which in turn causes the release of DA to the NAc under the control of α1ARs in the VTA (Park et al., 2017). Additionally, the α1bAR was found in glial elements in the NAc core and shell in this study. In other brain regions, it has been shown that NE (under the control of the α1AR) from the LC could cause glutamate release from astrocytes that in turn could affect release of other neurotransmitters, such as dopamine (Mitrano et al., 2016; Bazargani & Attwell,

2017). This also points to NE-DA interactions that need further examination in the NAc, as glial contributions to neurotransmission have become of increasing interest.

The importance of continuing to study the D1R and the α1bAR in the NAc is highlighted in the literature, especially in relation to their mechanisms of action and roles in response to psychostimulants. DA and D1Rs are at the root of maintaining drug self-administration and anticipation of a reward (Ritz et al., 1988; Kuhar et al., 1991; Dumartin et al., 1998; Koob & Volkow, 2016). On the other hand, NE and α1ARs have been implicated in various brain regions to be at the core of drug- and cue-induced reinstatement of drug-seeking behavior in cocaine self-administration studies (Schroeder et al., 2010; Schroeder et al., 2013; Schmidt et al., 2017; Solecki et al., 2017). In short, they have shown that lowering levels of NE or blockade of the α1AR can decrease reinstatement of cocaine-seeking behavior. Additionally, administration of the α1AR antagonist terazosin into the NAc shell attenuated cocaine-induced locomotor activity and increases in extracellular DA as measured by microdialysis (Mitrano et al., 2012).

In this study, a subtype specific antibody for the α1bAR showed a similar pattern of distribution as compared to using a pan-α1AR antibody (Mitrano et al., 2012), with slightly more dendrites and fewer spines immunoreactive for the α1bAR, but a high degree of presynaptic labeling, pointing to the α1bAR to be at the heart of the effects seen in the NAc from previous studies on NE and the D1R. For example, mice lacking the α1bAR showed decreased locomotor responses and behavioral sensitization to amphetamine, cocaine and morphine as well as decreased amphetamine-induced DA levels in the NAc without affecting D1Rs or dopamine reuptake transporter expression (Auclair et al., 2002; Drouin et al., 2002). α1bAR knockout mice treated with a DA reuptake transporter blocker and then exposed to enhanced NE release (using dexefaroxan, an α2AR antagonist), showed a substantial decrease in locomotor activity compared to wild-type mice, indicating that stimulating α1bARs causes an increase in DA-mediated responses, such as to amphetamine (Villegier et al., 2003). In cultured striatal neurons stimulated with DA, an α1AR agonist did not affect the resensitization rate as compared to cultured cortical neurons, which had an increased rate of resensitization of the D1R after agonist application (Trovero et al., 1994). These all indicate that the α1bAR and D1R are in opposing neurons; the effects are probably not due to receptor-receptor interactions within the postsynaptic element. Since the α1AR is found mainly presynaptically and with some frequency on dopaminergic terminals in the NAc and on GABAergic terminals (Mitrano et al., 2012) in the VTA (which in turn could modulate the activity of VTA dopaminergic neurons projecting to NAc; Park et al., 2017), it makes sense that manipulating the α1bAR could result in altered dopaminergic responses to psychostimulant drugs.

Attempts at understanding the localization and function of the α1bARs and D1Rs in the NAc have used various techniques other than electron microscopy. For example, methoxamine, the α1AR agonist, when injected into the NAc shell reduced extracellular DA efflux in freely moving rats but did not affect NE levels, effects that were reversed with application of the α1AR antagonist prazosin (Saigusa et al., 2012). This led the authors to conclude that the effects seen must be a result of the α1AR being located on noradrenergic and dopaminergic terminals in the NAc. Aono et al. (2015) showed that deactivation of the

α1bAR using a somewhat specific antagonist, cyclazosin, reversed the effect of the agonist methoxamine in the NAc by returning DA to basal levels. In the VTA, activation of α1ARs is necessary for cocaine-induced increases of dopamine seen in the NAc shell; indicating again that NE release from terminals can manipulate DA transmission (Goertz et al., 2015). All of these findings support an interaction of the noradrenergic and dopaminergic systems in the NAc and that perhaps the α1bAR is the prominent subtype in relation to these interactions.

Comparisons of α1bAR and D1R localization in the NAc and PFC

In the NAc, α1bARs and D1Rs colocalized in about 25–30% of dendrites, compared to the PFC, in which the α1bAR and D1R colocalized in about 60–70% of dendrites. In both brain regions, however, the receptors have altered subcellular localization when found together (Mitrano et al., 2014). When the α1bAR and D1R were found on the same PFC dendrites, there was a decreased presence of the α1bAR on the plasma membrane compared to dendrites that only contained the α1bAR; no difference was seen in the localization of the D1R when the receptors were found together (Mitrano et al., 2014). In the NAc shell, the opposite was seen in D1R-containing dendrites, unmyelinated axons, and axon terminals: increased expression of the α1bAR on the plasma membrane, only trends were seen for the NAc core. Additionally, in the NAc shell, the D1R had increased expression on the plasma membrane of spines and axon terminals when colocalized with α1bAR. While hard to interpret exactly what these findings mean, as using electron microscopy in both studies provides a single snapshot of these receptors in untreated animals, it is a limitation to this work. The high degree of intracellular receptors could imply many things, such as internalization of the receptors, trafficking of the receptors to and from the membrane or from the cell body. A high degree of PMB α1bARs on unmyelinated axons also raises many questions that are yet to be answered on their function; these could be pre-terminal axons that contribute to the modulation of neurotransmitter release on the terminals they are connected to, such as glutamate or dopamine. When found together, it is also hard to determine why there is a differential pattern of expression of the α1bAR and D1R in NAc compared to the PFC. Overall though, these findings infer some level of functional diversity and complexity in the responsiveness to NE and DA among neurons containing one receptor versus both, within the NAc and compared to the PFC.

Both the α1bAR and D1R are GPCRs, are coupled to different G-proteins and have their own unique dynamics in terms of desensitization and resensitization. Whether there are scaffolding proteins that link these receptors is still yet to be determined. Studies examining these receptors in an *in vivo* system in accumbal neurons is needed to shed light on activating one or both of the receptors and what functions they may have on the plasma membrane or intracellularly and whether their localization changes upon agonizing both receptors (with either endogenous ligands or indirectly with psychostimulants). Past studies used HEK-293 cells and showed the α1bAR was mainly on the plasma membrane but internalized quickly upon agonist application (Chalothorn et al., 2002). Other studies have shown that the D1R internalizes upon agonist application in an *in vivo* system (Dumartin et al., 1998); yet no studies have looked at both receptors at the same time.

Overall, these examples highlight the need to be able to distinguish amongst the three α1AR subtypes in order to gain a complete understanding of the NE-DA interactions that take place in the mesocorticolimbic circuitry. Important future experiments include examination of the α1bAR's presence on noradrenergic or other axon terminals in the NAc and examination of the circuitry between the PFC and NAc in relation to α1bARs.

In conclusion, the α1bAR and its colocalization with various receptors, such as the D1R, can vary from brain region to brain region. We have provided new anatomical evidence that sheds light on some functional studies showing interactions between these two receptors with respect to regulation of their neurotransmission. Additionally, this study explores one way to examine the different subtypes of the α1AR with the advent of new specific antibodies. While there have been attempts at developing subtype specific pharmacological agents for the α1bAR, such as cyclazosin, this compound has some activity at the α1dAR as well (Giardina et al., 1996, 2003). Therefore, this study shows the need to develop drugs that specifically target the various subtypes of the α1ARs, which may elucidate the complex modulation NE has on dopamine transmission. In addition, future work should look at possible changes in the localization of the α1bAR and D1Rs following stimulant administration to establish further evidence that a specific α1bAR antagonist may provide a new, more specific pharmacological target for preventing relapse in cocaine-and other stimulant-dependent individuals.

Acknowledgments

Christie Lacy for assistance at the University of Richmond Biological Imaging Lab; Ricardo Quintanilla for assistance in data analysis, Christopher Newport University; James W. Bogenpohl for editing this manuscript, Christopher Newport University.

Funding: This work was supported by Christopher Newport University Faculty Development Funds; Virginia Commonwealth University, Dept. of Anatomy & Neurobiology Microscopy Facility NIH-NINDS [Grant P30 NS047463] and NIH-NCI [Grant P30 CA016059]; Emory University, NIH-Animal Resources Program [Yerkes Base Grant P51OD011132].

Abbreviations

α1AR	alpha1-adrenergic receptor
α1bAR	alpha1b-adrenergic receptor
ANOVA	analysis of variance
ADHD	Attention Deficit Hyperactivity Disorder
ABC	avidin-biotin complex
BSA	bovine serum albumin
DAB	3,3-diaminobenzidine tetrahydrochloride
D1R	D1-dopamine receptor
DA	dopamine

GPCR	G-protein coupled receptor
HQ	high-quality silver enhancement
IgG	Immunoglobulin G
INT	intracellular
KO	knockout animal
LC	locus coeruleus
MW	molecular weight
NGS	normal goat serum
NE	norepinephrine
NAc	nucleus accumbens
PB	phosphate buffer
PBS	phosphate-buffered saline
PFC	prefrontal cortex
PMB	plasma membrane-bound
RT	room temperature
TBS	tris-buffered saline
VTA	ventral tegmental area

References

Aono Y, Taguchi H, Saigusa T, Uchida T, Takada K, Takiguchi H, Shirakawa T, Shimizu N, Koshikawa N, Cools AR. Simultaneous activation of the α1A-, α1B- and α1D-adrenoceptor subtypes in the nucleus accumbens reduces accumbal dopamine efflux in freely moving rats. Behav Pharmacol. 2015; 26:73–80. [PubMed: 25438092]

Arnsten AF, Li BM. Neurobiology of executive functions. Biol Psychiatry. 2005; 57:1377–84. [PubMed: 15950011]

Atzori M, Cuevas-Olguin R, Esquivel-Rendon E, Garcia-Oscos F, Salgado-Delgado RC, Saderi N, Miranda-Morales M, Treviño M, Pineda JC, Salgado H. Locus coeruleus norepinephrine release: A central regulator of CNS spatio-temporal activation? Front Synaptic Neurosci. 2016; 8:25. [PubMed: 27616990]

Auclair A, Cotecchia S, Glowinski J, Tassin JP. D-amphetamine fails to increase extracellular dopamine levels in mice lacking alpha 1b-adrenergic receptors: relationship between functional and nonfunctional dopamine release. J Neurosci. 2002; 22:9150–4. [PubMed: 12417637]

Bazargani N, Attwell D. Amines, astrocytes, and arousal. Neuron. 2017; 94:228–231. [PubMed: 28426956]

Bylund DB, Eikenberg DC, Hieble JP, Langer SZ, Lefkowitz RJ, Minneman KP, Molinoff PB, Ruffolo RR Jr, Trendelenburg U. International Union of Pharmacology nomenclature of adrenoceptors. Pharmacol Rev. 1994; 46:121–36. [PubMed: 7938162]

Center for Behavioral Health Statistics and Quality (NSDUH). Key substance use and mental health indicators in the United States: Results from the 2015 National Survey on Drug Use and Health (HHS Publication No. SMA 16-4984, NSDUH Series H-51). 2016.

Chalothorn D, McCune DF, Edelmann SE, García-Cazarín ML, Tsujimoto G, Piascik MT. Differences in the cellular localization and agonist-mediated internalization properties of the alpha (1)-adrenoceptor subtypes. Mol Pharmacol. 2002; 61:1008–16. [PubMed: 11961118]

Darracq L, Blanc G, Glowinski J, Tassin JP. Importance of the noradrenaline-dopamine coupling in the locomotor activating effects of D-amphetamine. J Neurosci. 1998; 18:2729–39. [PubMed: 9502830]

Drouin C, Darracq L, Trovero F, Blanc G, Glowinski J, Cotecchia S, Tassin JP. Alpha1b-adrenergic receptors control locomotor and rewarding effects of psychostimulants and opiates. J Neurosci. 2002; 22:2873–84. [PubMed: 11923452]

Dumartin B, Caillé I, Gonon F, Bloch B. Internalization of D1 dopamine receptor in striatal neurons in vivo as evidence of activation by dopamine agonists. J Neurosci. 1998; 18:1650–61. [PubMed: 9464990]

Gaval-Cruz M, Weinshenker D. Mechanisms of disulfiram-induced cocaine abstinence: antabuse and cocaine relapse. Mol Interv. 2009; 9:175–187. [PubMed: 19720750]

Giardina D, Crucianelli M, Romanelli R, Leonardi A, Poggesi E, Melchiorre C. Synthesis and biological profile of the enantiomers of [4-(4-amino-6,7-dimethoxyquinazolin-2-yl)-cis-octahydroquinoxalin-1-yl]furan-2-ylmethanone (cyclazosin), a potent competitive alpha 1B-adrenoceptor antagonist. J Med Chem. 1996; 39:4602–4607. [PubMed: 8917649]

Giardina D, Polimanti O, Sagratini G, Angeli P, Gulini U, Marucci G, Melchiorre C, Poggesi E, Leonardi A. Searching for cyclazosin analogues as alpha (1B)-adrenoreceptor antagonists. Farmaco. 2003; 58:477–487. [PubMed: 12818686]

Goertz RB, Wanat MJ, Gomez JA, Brown ZJ, Phillips PE, Paladini CA. Cocaine increases dopaminergic neuron and motor activity via midbrain α1 adrenergic signaling. Neuropsychopharmacology. 2015; 40:1151–1162. [PubMed: 25374094]

Goto Y, Yang CR, Otani S. Functional and dysfunctional synaptic plasticity in prefrontal cortex: roles in psychiatric disorders. Biol Psychiatry. 2010; 67:199–207. [PubMed: 19833323]

Hains AB, Arnsten AF. Molecular mechanisms of stress-induced prefrontal cortical impairment: implications for mental illness. Learn Mem. 2008; 15:551–564. [PubMed: 18685145]

Heal DJ, Cheetham SC, Smith SL. The neuropharmacology of ADHD drugs in vivo: insights on efficacy and safety. Neuropharmacology. 2009; 57:608–18. [PubMed: 19761781]

Hersch SM, Ciliax BJ, Gutekunst CA, Rees HD, Heilman CJ, Yung KK, Bolam JP, Ince E, Yi H, Levey AI. Electron microscopic analysis of D1 and D2 dopamine receptor proteins in the dorsal striatum and their synaptic relationships with motor corticostriatal afferents. J Neurosci. 1995; 15:5222–5237. [PubMed: 7623147]

Koob GF, Volkow ND. Neurobiology of addiction: a neurocircuitry analysis. Lancet Psychiatry. 2016; 8:760–773.

Kuhar MJ, Ritz MC, Boja JW. The dopamine hypothesis of the reinforcing properties of cocaine. Trends Neurosci. 1991; 14:299–302. [PubMed: 1719677]

Levey AI, Hersch SM, Rye DB, Sunahara RK, Niznik HB, Kitt CA, Price DL, Maggio R, Brann MR, Ciliax BJ. Localization of D1 and D2 dopamine receptors in brain with subtype-specific antibodies. Proc Natl Acad Sci USA. 1993; 90:8861–8865. [PubMed: 8415621]

Meredith GE, Pattiselanno A, Groenewegen HJ, Haber SN. Shell and core in monkey and human nucleus accumbens identified with antibodies to calbindin-D28k. J Comp Neurol. 1996; 365:628–639. [PubMed: 8742307]

Mitrano DA, Smith Y. Comparative analysis of the subcellular and subsynaptic localization of GluR1a and mGluR5 metabotropic glutamate receptors in the shell and core of the nucleus accumbens in rat and monkey. J Comp Neurol. 2007; 500:788–806. [PubMed: 17154259]

Mitrano DA, Ritter SL, Smith Y, Hall RA, Weinshenker D. Colocalization and interaction of D1 dopamine and alpha-1 adrenergic receptors in the rat prefrontal cortex. Society for Neuroscience Abstracts No. 844. 2010:28.

Mitrano DA, Schroeder JP, Smith Y, Cortright JJ, Bubula N, Vezina P, Weinshenker D. α1-adrenergic receptors are localized on presynaptic elements in the NAc and regulate mesolimbic dopamine transmission. Neuropsychopharmacology. 2012; 37:2161–2172. Cover. [PubMed: 22588352]

Mitrano DA, Pare JF, Smith Y, Weinshenker D. D1-dopamine and α1-adrenergic receptors co-localize in dendrites of the rat prefrontal cortex. Neuroscience. 2014; 258:90–100. [PubMed: 24231738]

Mitrano, DA., Fekir, S., Odil, L., Weinshenker, D. Society for Neuroscience Abstracts No.135.08. 2016. A locus coeruleus-ventral periaqueductal gray arousal circuit: Subcellular localization of the alpha-1 adrenergic receptor.

Pan WH, Yang SY, Lin SK. Neurochemical interaction between dopaminergic and noradrenergic neurons in the medial prefrontal cortex. Synapse. 2004; 53:44–52. [PubMed: 15150740]

Park JW, Bhimani RV, Park J. Noradrenergic modulation of dopamine transmission evoked by electrical stimulation of the locus coeruleus in rat brain. ACS Chem Neurosci. 2017; [Epub ahead of print]. doi: 10.1021/acschemneuro.7b00078

Paxinos, G., Watson, C. The rat brain in stereotaxic coordinates. London: Academic Press Ltd; 1998.

Peters, A., Palay, S., Webster, HD. The fine structure of the nervous system: neurons and their supporting cells. New York: Oxford University Press; 1991.

Ritz MC, Lamb RJ, Goldberg SR, Kuhar MJ. Cocaine self-administration appears to be mediated by dopamine uptake inhibition. Prog in Neuropsychopharmacol & Biol Psychiatry. 1988; 12:233–239. [PubMed: 3387585]

Ritz MC, Kuhar MJ. Relationship between self-administration of amphetamine and monoamine receptors in brain: comparison with cocaine. J Pharmacol Exp Ther. 1989; 248:1010–7. [PubMed: 2703961]

Saigusa T, Aono Y, Uchida T, Takada K, Verheij MM, Koshikawa N, Cools AR. The α_1-, but not α_2-, adrenoceptor in the nucleus accumbens plays an inhibitory role upon the accumbal noradrenaline and dopamine efflux of freely moving rats. Eur J Pharmacol. 2012; 688:35–41. [PubMed: 22617026]

Schmidt KT, Weinshenker D. Adrenaline rush: The role of adrenergic receptors in stimulant-induced behaviors. Mol Pharmacol. 2014; 85:640–650. [PubMed: 24499709]

Schmidt KT, Schroeder JP, Foster SL, Squires K, Smith BM, Pitts EG, Epstein MP, Weinshenker D. Norepinephrine regulates cocaine-primed reinstatement via α1-adrenergic receptors in the medial prefrontal cortex. Neuropharmacology. 2017; 119:134–140. [PubMed: 28392265]

Schroeder JP, Cooper DA, Schank JR, Lyle MA, Gaval-Cruz M, Ogbonmwan YE, Pozdeyev N, Freeman KG, Iuvone PM, Edwards GL, Holmes PV, Weinshenker D. Disulfiram attenuates drug-primed reinstatement of cocaine seeking via inhibition of dopamine β-hydroxylase. Neuropsychopharmacology. 2010; 35:2440–2449. [PubMed: 20736996]

Schroeder JP, Alisha Epps S, Grice TW, Weinshenker D. The selective dopamine b-hydroxylase inhibitor nepicastat attenuates multiple aspects of cocaine-seeking behavior. Neuropsychopharmacology. 2013; 38:1032–1038. [PubMed: 23303068]

Solecki WB, Szklarczyk K, Pradel K, Kwiatkowska K, Dobrzański G, Przewłocki R. Noradrenergic signaling in the VTA modulates cocaine craving. Addict Biol. 2017; [Epub ahead of print]. doi: 10.1111/adb.12514

Stojanovic T, Orlova M, Sialana FJ, Hoger H, Stuchlik S, Milenkovic I, Aradska J, Lubec G. Validation of dopamine receptor DRD1 and DRD2 antibodies using receptor deficient mice. Amino Acids. 2017; 49:1101–1109. [PubMed: 28316027]

Trovero F, Marin P, Tassin JP, Premont J, Glowinski J. Accelerated resensitization of the D1 dopamine receptor-mediated response in cultured cortical and striatal neurons from the rat. J Neurosci. 1994; 14:6280–6288. [PubMed: 7931580]

Vicentic A, Robeva A, Rogge G, Uberti M, Minneman KP. Biochemistry and pharmacology of epitope-tagged α1-adrenergic receptor subtypes. J Pharmacol Exp Ther. 2002; 302:58–62. [PubMed: 12065700]

Villegier A-S, Drouin C, Bizot J-C, Marien M, Glowinski J, Colpaert F, Tassin J-P. Stimulation of postsynaptic α1b- and α2- adrenergic receptors amplifies dopamine-mediated locomotor activity in both rats and mice. Synapse. 2003; 50:277–284. [PubMed: 14556232]

Visser SN, Danielson ML, Bitsko RH, Holbrook JR, Kogan MD, Ghandour RM, Perou R, Blumberg SJ. Trends in the parent-report of health care provider-diagnosed and medicated Attention-Deficit/Hyperactivity Disorder: United States, 2003–2011. J Am Acad Child Adolesc Psychiatry. 2014; 53:34–46. [PubMed: 24342384]

Weinshenker D, Schroeder J. There and back again: A tale of norepinephrine and drug addiction. Neuropsychopharmacology. 2007; 32:1433–1451. [PubMed: 17164822]

Wise RA, Bozarth MA. Brain mechanisms of drug reward and euphoria. Psychiatr Med. 1985; 3:445–60. [PubMed: 2893431]

Wise RA, Bozarth MA. A psychomotor stimulant theory of addiction. Psychol Rev. 1987; 94:469–492. [PubMed: 3317472]

Yun J, Gaivin RJ, McCune DF, Boongird A, Papay RS, Ying Z, Gonzalez-Cabrera PJ, Najm I, Perez DM. Gene expression profile of neurodegeneration induced by α_{1B}-adrenergic receptor overactivity: NMDA/GABAA dysregulation and apoptosis. Brain. 2003; 126:2667–81. [PubMed: 12937073]

Zahm DS, Brog JS. On the significance of subterritories in the “accumbens” part of the rat ventral striatum. Neuroscience. 1992; 50:751–767. [PubMed: 1448200]

Zhang XY, Kosten TA. Prazosin, an alpha-1 adrenergic antagonist, reduces cocaine-induced reinstatement of drug-seeking. Biol Psychiatry. 2005; 57:1202–1204. [PubMed: 15866561]

Zhong H, Minneman KP. Alpha1-adrenoceptor subtypes. Eur J Pharmacol. 1999; 375:261–76. [PubMed: 10443582]

Zuscik MJ, Sands S, Ross SA, Waugh DJ, Gaivin RJ, Morilak D, Perez DM. Overexpression of the α_{1B}-adrenergic receptor causes apoptotic neurodegeneration: multiple system atrophy. Nat Med. 2000; 6:1388–94. [PubMed: 11100125]

Highlights

- The subtype of the α1-adrenergic receptor, α1bAR, is found presynaptically in the nucleus accumbens core and shell.
- α1bARs and D1-dopamine receptors have minimal colocalization in dendrites in these brain regions.
- Colocalization of these receptors is greater when comparing the nucleus accumbens to the prefrontal cortex.
- Anatomical data presented here correlates with previous functional studies of these receptors in the nucleus accumbens.

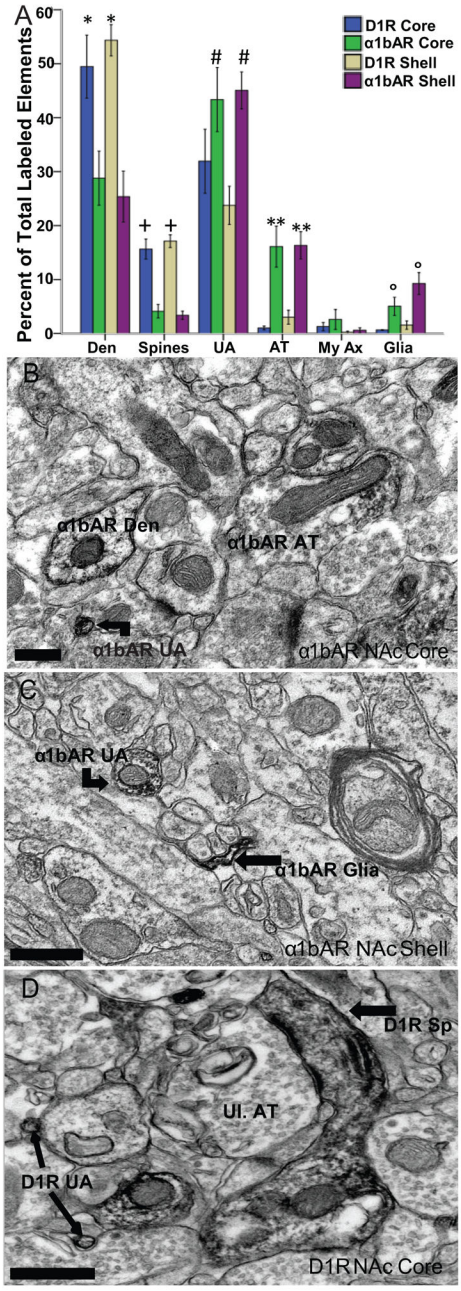

Figure 1.

Subcellular localization of D1Rs and α1bARs in the core and shell of the NAc. (A) Mean ± SEM of total D1R- or α1bAR-immunolabeled elements in the core and shell of the NAc using the single pre-embedding immunoperoxidase method. *p<0.01 when comparing D1R-containing dendrites to α1bAR-labeled dendrites in the core and shell. +p<0.001 when comparing D1R spines to α1bAR spines. #p<0.05 when comparing α1bAR-labeled unmyelinated axons to D1R axons. **p<0.001 when comparing α1bAR-labeled axon terminals to D1R terminals and °p<0.01 when comparing α1bAR-labeled glial elements to D1R glia. (B) Representative electron micrograph of α1bAR labeling in a dendrite,

unmyelinated axon and an axon terminal in the NAc core. (C) Representative electron micrograph of α1bAR labeling in an unmyelinated axon and glial process in the NAc shell. (D) Representative electron micrograph of D1R labeling in 2 unmyelinated axons, 2 dendrites, one with a protruding spine synapsing on an unlabeled axon terminal. Den, dendrite; Sp, dendritic spine; UA, unmyelinated axon; AT, axon terminal; Ul., unlabeled. All scale bars = 0.5μm.

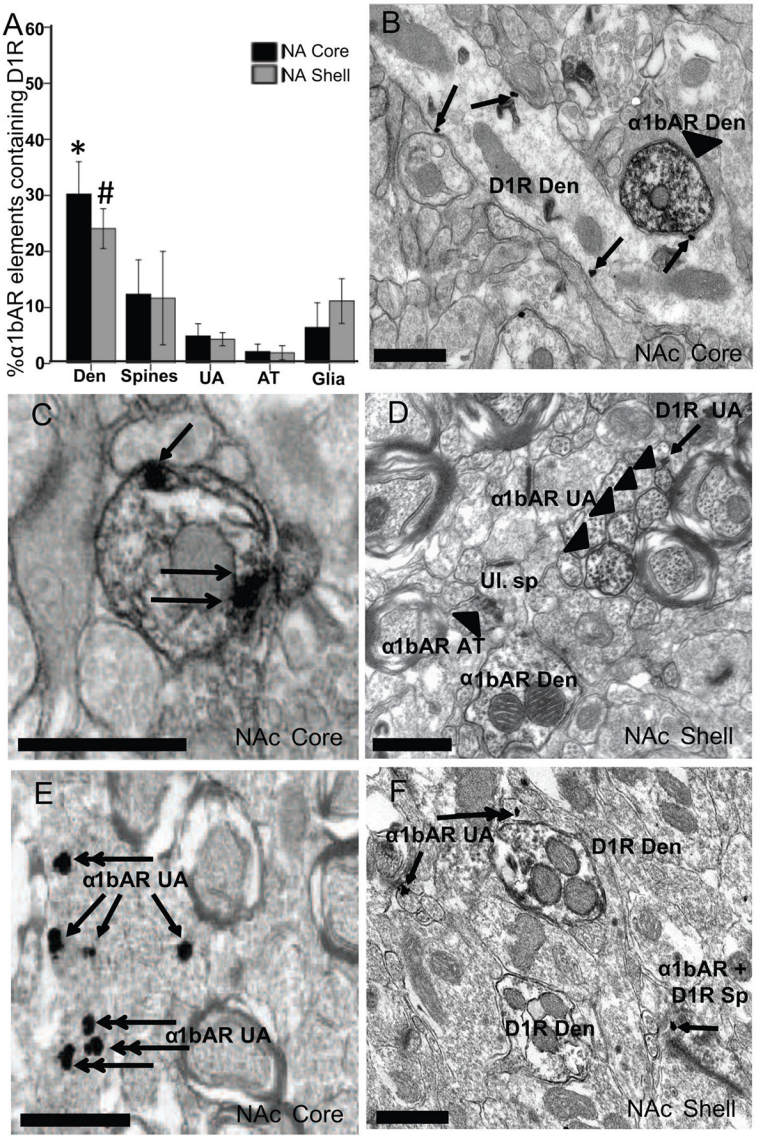

Figure 2.

α1bAR and D1R display a low degree of colocalization in the core and shell of the NAc. (A) The mean percent (± SEM) of α1bAR immunoperoxidase-containing elements that also contained immunogold labeling representing the D1R in both the core and shell of the NAc. *$p<0.01$ indicates in the NAc core, a significantly greater percentage of double-labeled dendrites vs. unmyelinated axons, axon terminals and glial elements. #$p<0.05$ indicates in the NAc shell, significantly more double-labeled dendrites than unmyelinated axons and axon terminals. (B) Representative electron micrograph from the NAc core with an immunoperoxidase-labeled dendrite representing α1bAR (arrowhead) and a D1R labeled dendrite (arrows point to PMB immunogold particles). (C) Electron micrograph of an immunoperoxidase-labeled α1bAR dendrite containing D1R PMB immunogold particles (arrows). (D) NAc shell, 4 α1bAR immunoperoxidase-labeled unmyelinated axons, α1bAR axon terminal (arrowhead), α1bAR dendrite with an unlabeled protruding spine. The single

arrow points to a D1R-labeled unmyelinated axon immunogold particle. (E) Representative electron micrograph from the NAc core with α1bAR immunogold-labeled unmyelinated axons (single arrows point to PMB gold particles, double arrowhead indicates INT gold particles). (F) Electron micrograph from the NAc shell with 2 D1R immunoperoxidase-labeled dendrites, 2 α1bAR immunogold-labeled unmyelinated axons and one spine containing D1R immunoperoxidase labeling and immunogold labeling for the α1bAR (single arrows point to PMB gold particles, double arrowhead indicates INT gold particles). Den, dendrite; Sp, dendritic spine; UA, unmyelinated axon; AT, axon terminal; Ul., unlabeled. All scale bars = 0.5μm.

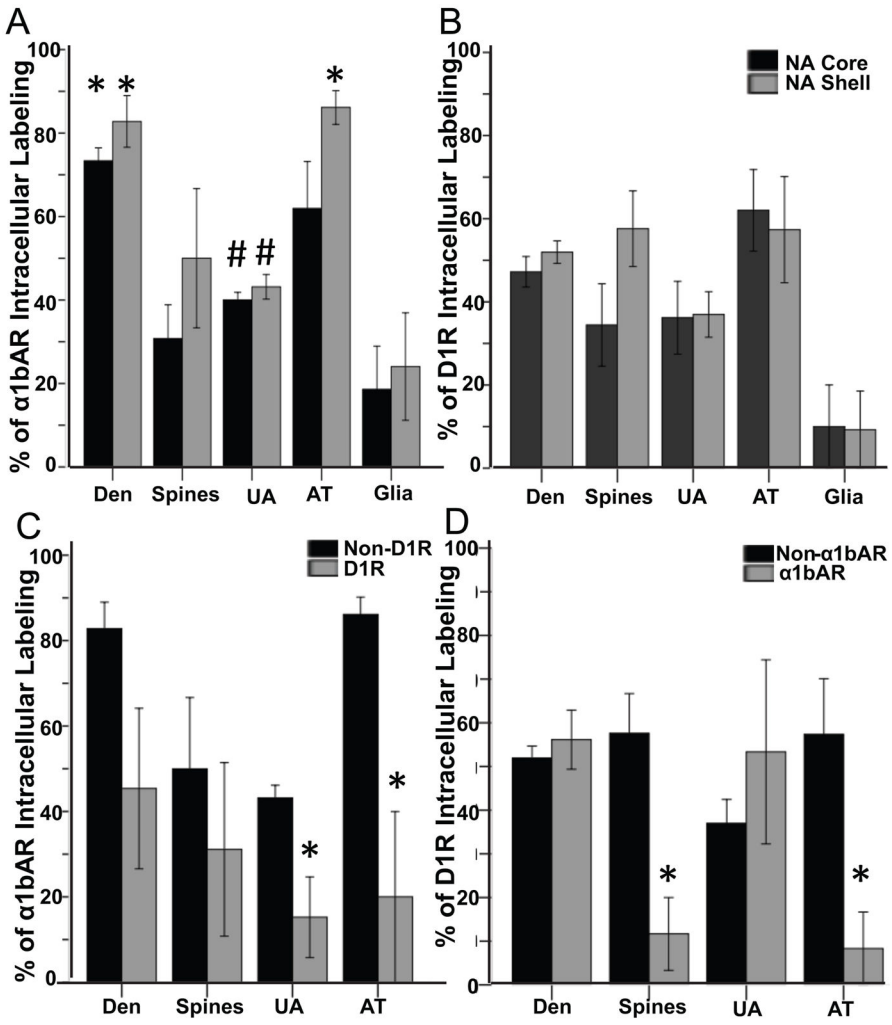

Figure 3.

Subsynaptic Distribution of α1bARs and D1Rs. (A) The mean percent (+/− SEM) of intracellular immunogold particles representing α1bARs in the NAc core and shell. *p<0.001 when comparing the mean percent intracellular immunogold particles to PMB particles on dendrites in both the core and shell; for axon terminals in the shell only. #p<0.01 when comparing the mean percent of intracellular to PMB gold particles in unmyelinated axons. Total number of elements examined containing only α1bAR immunogold: 69 dendrites (core), 52 (shell); 12 spines (core), 10 (shell); 189 unmyelinated axons (core), 141 (shell); 48 axon terminals (core), 50 (shell); 10 glial elements (core), 12 (shell). (B) The mean percent (+/− SEM) of intracellular immunogold particles representing D1Rs in the NAc core and shell. Total number of elements examined containing only D1R immunogold: 252 dendrites (core), 229 (shell); 76 spines (core), 56 (shell); 137 unmyelinated axons (core), 139 (shell); 21 axon terminals (core), 33 (shell); 3 glial elements (core), 4 (shell). (C) Mean percent (+/−SEM) of intracellular immunogold particles representing the α1bAR in single (Non-D1R) vs. double labeled elements (D1R) in the NAc shell; *p<0.05 when comparing intracellular immunogold particles for α1bAR in Non-D1R vs. D1R-containing elements. Total number of elements examined containing both α1bAR immunogold and

D1R immunoperoxidase in the NAc shell: 77 dendrites; 12 spines; 21 unmyelinated axons; 17 axon terminals. (D) Mean percent (+/−SEM) of intracellular immunogold particles representing the D1R in single (Non-α1bAR) vs. double labeled elements (α1bAR) in the NAc shell; *$p<0.01$ when comparing intracellular immunogold particles for D1R in Non-α1bAR vs. α1bAR -containing elements. Total number of elements examined containing both D1R immunogold and α1bAR peroxidase in the NAc shell: 47 dendrites; 2 spines; 13 unmyelinated axons; 2 axon terminals.

Table 1

Primary antibodies used for immunocytochemistry

Antigen	Immunogen	Manufacturer Data	Dilution Used
α1bAR	15 amino acid peptide from the C-terminal residues of human α1bAR.	Abcam, Rabbit Polyclonal, #ab84405, RRID:AB_1859856	1:3000
D1R	Recombinant fusion protein containing the C-terminal 97 amino acids of human D1 receptor.	Sigma-Aldrich, Rat, Monoclonal, #D2944, RRID:AB_1840787	1:750